

THEORETICAL STUDIES OF NEGATIVE MOLECULAR IONS

❖ 2637

Jack Simons¹

Department of Chemistry, The University of Utah, Salt Lake City, Utah 84112

INTRODUCTION

In 1968 Berry (1) reviewed the experimental and theoretical progress that had been made toward understanding the stabilities and bonding characteristics of small, isolated (gas phase), negative ions. In this review Berry commented:

For the theorist, electron affinities and other properties of negative ions pose greater difficulties than do properties of neutrals or positives, insofar as electron correlation plays a relatively larger part in determining the properties of a negative ion than it does in other species. In fact, electron affinities are frequently about the same size as the differences between correlation energies in atoms and in the corresponding negative ions.

As an example of the magnitude of electron correlation effects, one need only consider the results of our calculations on the vertical ($R = 1.718$ au) electron detachment energy ($X^1\Sigma^+OH^- \rightarrow X^2\Pi,OH$) of OH^- . Using an atomic orbital basis consisting of 20 Slater-type orbitals (STOs), we obtained a Koopmans' theorem approximation to the detachment energy equal to 3.06 eV. The energy difference between two separate SCF calculations (Δ SCF), one on OH^- and one on OH , carried out within the same basis, was equal to -0.2 eV. The difference between Koopmans' theorem and Δ SCF represents the effects of allowing the orbitals to relax upon removal of the π electron. Our best computed energy difference (2), which contains effects of electron correlation through third order, was 1.76 eV, which is in good agreement with both Branscomb's early experiments (3) and Lineberger's more recent laser detachment results (4). The difference between 1.76 eV and the Δ SCF value of -0.2 eV represents the effects of electron correlation. These effects are indeed as large as the entire electron affinity of OH ; moreover, this result is not atypical.

¹ Alfred P. Sloan Foundation Fellow, Camille and Henry Dreyfus Fellow.

Because the treatment of both orbital relaxation and electron correlation effects in a sufficiently rigorous manner is an absolute necessity in any reliable scheme for computing properties of anions, theoretical progress toward understanding negative ions has been made rather slowly. Quite simply put, it is difficult to include correlation effects to a high enough order to guarantee precision of ± 0.2 eV in computed ion-neutral energy differences. In Berry's review article, his assessment of the state of quantum chemical research on anions involved briefly mentioning the works of Pekeris (5) on H^- ; Weiss (6) on Li^- , Na^- , and K^- ; Clementi and co-workers (7) on several atomic ions; Sinanoglu (8) on C^- , O^- , and F^- ; Taylor & Harris (9) on H_2^- ; Wahl & Gilbert (10) on halogen diatomics; and Cade (11) on OH^- , CH^- , SiH^- , SH^- , and PH^- . Therefore, in 1968 it would have been fair to say that negative molecular ions could not yet be conveniently studied by existing quantum chemical methods. On the other hand, the development of modern laser technology was making new tools available to the experimentalist to use in carrying out high-precision photodetachment and photoelectron spectroscopy studies of gas-phase anions. Thus, even in 1968 a great deal of experimental progress had begun. These experimental developments made the parallel development of theoretical methods and models aimed at better understanding negative ions a necessary and quite natural step in the scientific progress in this area.

In 1973 Simons & Smith (12) published an article in which they attempted to use equation-of-motion (EOM) techniques to express the vertical electron affinity (EA) or detachment energy (DE) of a closed-shell species in a manner that treated orbital relaxation and electron correlation through third order in perturbation theory (the difference between the coulombic interaction and the Hartree-Fock interaction is the perturbation). This developmental paper was followed by other formal papers by Simons, Jørgensen, Jordan, and Chen (13–15) in which small deficiencies in the original theory were corrected and connection made with the recent Green's function developments of Cederbaum (16), Pickup & Goscinski (17), Purvis & Öhrn (18), and Freed (19). The result of these papers was a method that permits the direct calculations of EAs and DEs of closed-shell species, which are accurate through third order.

In succeeding publications (2, 20–26), the third-order EOM theory was applied to studies of the stability and bonding characteristics of several molecular anions (and cations). Calculations of the electron affinities of OH , BeH , NH_2 , CN , and BH provided theoretical support (to within ± 0.2 eV) for existing experimental measurements. Studies of the EAs of BO and Li_2 resulted in theoretical predictions for species where good experimental data is not available. Calculations of the EAs of LiF , $LiCl$, LiH , NaH , and BeO have led to predictions of both the existence and the stabilities (with respect to electron loss) of the anions of these species. Jordan (92) has also examined the dimer anion $(LiH)_2^-$; Simons & Jordan (93) have recently found Be_2^- to be stable even though Be_2 is unbound. Very recently, the ion $LiCl^-$ was observed by Lineberger (27), thereby verifying the theoretical prediction of Jordan et al (77). Later in this review we treat the precise nature of some of the calculations mentioned above, together with the principal conclusions of these works.

In the time since Berry's 1968 review article was completed as well as for a few years previously, several ab initio calculations, in addition to those mentioned above, were performed on molecular anions that are of chemical interest. These studies include the following works: Clementi (28) (N_3^-), Lipscomb (29) (PO^-), Krauss (30) (BH_4^- , O_2^-), Kaufman (31) (O_3^-), Csizmadia (32) (CH_3^- , NH_2^-), Pfeiffer (33) (NO_2^-), Popkie (34) (C_2^-), McLean (35) (OCN^- , SCN^-), Wahl (36) (Cl_2^- , F_2^-), Fink (37) (OH^- , NH_2^- , CH_3^- , BH_4^-), Geller (38) (BH_2^-), Thulstrup (39) (NO^-), Peyerimhoff (40) (BeH_3^-), Heaton (41) (NH_2^-), Schaefer (42) (NO_2^-), Thulstrup (84) (C_2^-), O'Hare (85) (NF^- , NS^- , PF^- , SF^-).

The above list is by no means a complete tabulation of all work done on negative molecular ions; it is simply meant to indicate the kinds of systems that have been studied as well as the approximate number of calculations that have been performed to date. Although it is true that a reasonably large number of ab initio calculations have been carried out for diatomic and small polyatomic species, very few of the studies listed above include any electron correlation effects. Most of these calculations have been done at the SCF level within small- to moderate-size bases. Therefore, the EAs that have been obtained in this manner are probably not reliable. On the other hand, the equilibrium geometries and charge densities obtained in the above SCF-level works may not be any less accurate than the results of analogous calculations on neutral species; electron correlation effects are not as dominant in determining charge densities and geometries as they are in determining EAs. Nevertheless, it is my feeling that most of the reliable work on negative ions has been, and will continue to be, characterized by a careful treatment of electron correlation and charge relaxation. For this reason, the remainder of this review will be restricted to discussion of results of studies which treat correlation in an ab initio manner.

With this brief survey of the developments made since 1968 as a background, let us now turn to a more detailed discussion of the most recently utilized methods as well as of the results that have been obtained with these methods. In the following section we review the foundation of the direct-calculation approach of References 12-19. The third section of this review contains a survey of results on OH^- , NH_2^- , BeH^- , MgH^- , CN^- , BO^- , LiF^- , LiCl^- , LiH^- , NaH^- , BeO^- , and NO_2^- , in which the effects of orbital relaxation and correlation have been included. Specific attention is paid to stabilities (EA or DE), geometries (R_e , θ_e), vibrational frequencies, dissociation energies, and charge densities. In the final section we review the conclusions that have been reached thus far, and we suggest areas which seem to show special promise for future development.

THEORETICAL METHODS

The electron propagator, or the one-electron Green's function (15), has been used for some time (16, 18, 20-26, 43-46) in the study of electron spectroscopy. The advantages of using the electron propagator arise because the transition energies and the transition strengths are obtained directly as poles and residues of the propagator, respectively. Several alternative procedures for decoupling the equation of

motion (EOM) for the electron propagator have been developed. In this work we use the superoperator formalism of Goscinski & Lukman (47) as the framework for our development of an electron propagator that is consistent through third order. In an alternative derivation using the equation-of-motion formalism of Rowe (48), Simons & Smith (12) attempted to obtain an equation of motion that was consistent through third order. Purvis & Öhrn (49) pointed out some deficiencies in the theory of Simons & Smith; these deficiencies are mentioned again in this section. We show further how the electron propagator can be obtained consistent through third order. The consistency is made more apparent by demonstrating that all second- and third-order self-energy diagrams of Cederbaum (16) are included in our formalism.

The definition of the spectral electron propagator (44) can be written within the superoperator formalism as

$$\mathbf{G}(E) = [\mathbf{a}|(E\hat{I} - \hat{H})^{-1}|\mathbf{a}], \quad 1.$$

where \hat{I} and \hat{H} are the superoperator identity and Hamiltonian respectively, and the \mathbf{a} are a set of annihilation operators $\mathbf{a} = \{a_i\}$ that are arranged in a superrow vector. The superoperator scalar product is defined in the conventional fashion (47). The superoperator resolvent $(E\hat{I} - \hat{H})^{-1}$ can be approximated via the inner projection technique, and the propagator then takes the form

$$\mathbf{G}(E) = (\mathbf{a}|\mathbf{h})(\mathbf{h}|E\hat{I} - \hat{H}|\mathbf{h})^{-1}(\mathbf{h}|\mathbf{a}), \quad 2.$$

where \mathbf{h} is a projection manifold that, if chosen to be complete and orthonormal, makes Equations 1 and 2 identical. The operator space

$$\{\mathbf{h}_1, \mathbf{h}_3, \mathbf{h}_5 \dots\} = \{a_i, a_i^\dagger a_k a_l, a_i^\dagger a_j^- a_k a_l, \dots\}, k > l, i > j, k > l > r \dots \quad 3.$$

spans the manifold \mathbf{h} . We now discuss appropriate selections of \mathbf{h} that, in conjunction with our choice of the reference state, ensure that the electron propagator is calculated correctly through third order in the electronic interaction.

It is well known (17, 45) that the projection manifold $\mathbf{h}_1, \mathbf{h}_3$, in connection with the Hartree-Fock (HF) ground state, is able to give the electron propagator correct through second order in the electronic interaction. Our experience (2, 20–26) tells us that second-order calculation of EAs is not sufficiently precise to be useful, except in well-understood special cases that are discussed below. We demonstrate how, using a correlated ground state and the same projection manifold, we are able to get the electron propagator correct through third order in the electronic interaction.

The effect of including \mathbf{h}_5 in the projection manifold, where the HF ground state is used as reference state, has been discussed by Tyner et al (50), and from their analysis it is clear that \mathbf{h}_5 introduces terms that are at least fourth order in the electronic interaction, independent of the choice of reference state. We therefore concentrate on using $\mathbf{h}_1, \mathbf{h}_3$ as our projection manifold in our search for a theory that is consistent through third order.

As the reference state in our analysis we use a correlated wave function given by:

$$|0\rangle = N^{-1/2} \left\{ 1 + \sum_{p\delta} (K_{\delta p}^p a_p^+ a_\delta) + \sum_{\substack{m>n \\ \alpha>\beta}} (K_{\alpha\beta}^{mn} a_m^+ a_n^+ a_\beta a_\alpha) \right. \\ \left. + \sum_{\substack{m>n>p \\ \alpha>\beta>\delta}} (K_{\alpha\beta\delta}^{mnp} a_m^+ a_n^+ a_p^+ a_\alpha a_\beta a_\delta) + \dots \right\} |HF\rangle, \quad 4.$$

where the a^+ are a set of HF creation operators, and where indices m, n, p, q ($\alpha, \beta, \delta, \gamma$) refer to unoccupied (occupied) spin orbitals in the HF ground state, and i, j, k, l, r are unspecified spin orbitals. We take the correlation coefficients from Rayleigh-Schrödinger perturbation theory:

$$K_{\delta p}^p = \sum_{\substack{m>n \\ \alpha>\beta}} \{ \langle p\alpha | mn \rangle \delta_{\delta\beta} - \langle p\beta | mn \rangle \delta_{\alpha\delta} + \langle \beta\alpha | \delta m \rangle \delta_{np} - \langle \beta\alpha | \delta n \rangle \delta_{pm} \} \\ \times \frac{\langle mn | \alpha\beta \rangle}{(\epsilon_\delta - \epsilon_p)(\epsilon_\alpha + \epsilon_\beta - \epsilon_n - \epsilon_m)} + \text{higher order terms in the electronic interaction} = K_{\delta p}^p(2, 3, \dots), \quad 5.$$

$$K_{\alpha\beta}^{mn} = \frac{\langle mn | \alpha\beta \rangle}{\epsilon_\alpha + \epsilon_\beta - \epsilon_m - \epsilon_n} + \text{higher order terms in the electronic interaction} = K_{\alpha\beta}^{mn}(1, 2, \dots), \quad 6.$$

$$K_{\alpha\beta\delta}^{mnp} = K_{\alpha\beta\delta}^{mnp}(2, 3, \dots), \quad 7.$$

where the first number in the bracket indicates the lowest order in the electronic interaction. The ϵ_i indicate HF orbital energies, and the two-electron integral $\langle mn | \alpha\beta \rangle$ refers to the charge densities $m\alpha$ and $n\beta$; we have

$$\langle mn | \alpha\beta \rangle = \langle mn | \alpha\beta \rangle - \langle mn | \beta\alpha \rangle. \quad 8.$$

In our analysis we consider the projection manifold $\{\mathbf{h}_1, \mathbf{h}_3\}$, where the \mathbf{h}_3 space has been redefined for convenience as

$$\mathbf{h}_3 = \{a_i^+ a_k a_l + \langle a_i^+ a_l \rangle a_k - \langle a_i^+ a_k \rangle a_l\}. \quad 9.$$

The choice of the subspace \mathbf{h}_3 ensures that this space is orthogonal to \mathbf{h}_1 :

$$(\mathbf{h}_1 | \mathbf{h}_3) = 0, \quad 10.$$

even for a correlated reference state. We also have the following orthogonality relations:

$$(\mathbf{h}_1 | \mathbf{h}_1) = 1, \quad (\mathbf{h}_3 | \mathbf{h}_3) = S(0, 2, 3, \dots). \quad 11.$$

Using Equations 10 and 11, Equation 2 can be partitioned into the form

$$\mathbf{G}^{-1}(E) = (\mathbf{h}_1 | E\hat{I} - \hat{H} | \mathbf{h}_1) - (h_1 | \hat{H} | \mathbf{h}_3)(\mathbf{h}_3 | \hat{E}I - \hat{H} | \mathbf{h}_3)^{-1}(\mathbf{h}_3 | \hat{H} | h_1) \\ = E\mathbf{1} - \mathbf{A} - \mathbf{B}\mathbf{D}^{-1}\mathbf{C}, \quad 12.$$

where the matrices **A**, **B**, **C**, and **D** are defined as:

$$\begin{aligned} \mathbf{A} &= (\mathbf{h}_1 | \hat{H} | \mathbf{h}_1), \\ \mathbf{B} &= (\mathbf{h}_1 | \hat{H} | \mathbf{h}_3), \\ \mathbf{C} &= (\mathbf{h}_3 | \hat{H} | \mathbf{h}_1), \\ \mathbf{D} &= (\mathbf{h}_3 | E\hat{I} - \hat{H} | \mathbf{h}_3), \end{aligned} \quad 13.$$

We will now make an order-by-order analysis of Equation 12, in which we retain only those terms that are zeroth, first, second, or third order in the electronic interaction. Since the **B** and **C** matrices are at least of first order (12), we need to consider only that part of the **D** matrix that is zeroth and first order. This constrains the indices in the projection manifold \mathbf{h}_3 to be of the form $a_m^+ a_\alpha a_\beta > \beta$ or $a_\alpha^+ a_m a_n > n$, since operators such as $a_m^+ a_n a_\alpha$ lead to matrix elements in the **D** matrix that are at least of second order. The resulting subspace \mathbf{h}_3 is thus identical to that used in calculating the electron propagator correctly through second order. To calculate the the electron propagator through third order in the electron repulsions, we thus need to obtain the **B** and **C** matrices through second order, the **D** matrix through first order, and the **A** matrix through third order.

Previous attempts (12) to obtain the electron propagator correctly through third order have used as the reference state:

$$|0\rangle = N_0^{-1/2} \left(1 + \sum_{\substack{m>n \\ \alpha>\beta}} K_{\alpha\beta}^{mn} a_m^+ a_n^+ a_\alpha a_\beta \right) |HF\rangle, \quad 14.$$

where the $K_{\alpha\beta}^{mn}$ are determined from first order Rayleigh-Schrödinger perturbation theory. In calculating the **B**, (**C**), and **D** matrix elements correctly through second and first order, respectively, no changes are obtained from considering the higher correlated ground state in Equation 4. The matrix elements of **B**, **C**, and **D** are given by:

$$B_{i,\alpha m\beta} = -\langle im|\alpha\beta\rangle - 1/2 \sum_{p,q} \langle im|pq\rangle K_{\alpha\beta}^{pq} + \sum_{\gamma,p} [\langle i\gamma|p\alpha\rangle K_{\beta\gamma}^{mp} - \langle i\gamma|p\beta\rangle K_{\alpha\gamma}^{mp}], \quad 15.$$

$$B_{i,\alpha m} = \langle i\alpha|mm\rangle + 1/2 \sum_{\gamma\delta} \langle i\alpha|\delta\gamma\rangle K_{\delta\gamma}^{mn} + \sum_{\gamma p} [\langle ip|\gamma n\rangle K_{\alpha\gamma}^{mp} - \langle ip|\gamma m\rangle K_{\alpha\gamma}^{np}], \quad 16.$$

$$\mathbf{C}^+ = \mathbf{B} \text{ (through second order)}. \quad 17.$$

$$D_{n\alpha m,\delta p\gamma} = 0, \quad 18.$$

$$\begin{aligned} D_{n\alpha m,q\beta p} &= \delta_{nq}\delta_{\alpha\beta}\delta_{mp}(\epsilon_m + \epsilon_n - \epsilon_\alpha) - \delta_{qn}\langle m\beta||p\alpha\rangle - \delta_{pm}\langle n\beta||q\alpha\rangle \\ &\quad + \delta_{qm}\langle n\beta||p\alpha\rangle + \delta_{\alpha\beta}\langle mn||pq\rangle + \delta_{pn}\langle m\beta||q\alpha\rangle, \end{aligned} \quad 19.$$

$$\begin{aligned} D_{\delta p\gamma,\alpha\beta} &= -\{\delta_{\delta\alpha}\delta_{p\alpha}\delta_{\gamma\beta}(\epsilon_p - \epsilon_\delta - \epsilon_\gamma) - \delta_{\gamma\beta}\langle \delta q||\alpha p\rangle - \delta_{\delta\alpha}\langle \gamma q||\beta p\rangle \\ &\quad + \delta_{\gamma\alpha}\langle \delta q||\beta p\rangle - \delta_{p\alpha}\langle \delta\gamma||\beta\alpha\rangle + \delta_{\delta\beta}\langle \gamma q||\alpha p\rangle\}. \end{aligned} \quad 20.$$

In the **A** matrix we need to include all terms up to third order. The **A** matrix elements obtained by using the state defined in Equation 14 as a reference state need to be modified by third-order terms that result from interaction between the singly excited states and the HF ground state. The triply excited states that also result from a

second-order Rayleigh-Schrödinger perturbation calculation do not introduce third-order terms. We thus have to add to the A matrix elements given in Reference 12 the terms δA_{ij} defined by:

$$\delta A_{ij} = \sum_{\substack{\delta\beta \\ pmn}} \frac{\langle jp||i\delta\rangle\langle\delta\beta||mn\rangle\langle mn||p\beta\rangle}{(\varepsilon_\delta - \varepsilon_p)(\varepsilon_\delta + \varepsilon_\beta - \varepsilon_m - \varepsilon_n)}, \quad (\text{A3})$$

$$+ \sum_{\substack{\delta\beta \\ pmn}} \frac{\langle j\delta||ip\rangle\langle p\beta||mn\rangle\langle mn||\delta\beta\rangle}{(\varepsilon_\delta - \varepsilon_p)(\varepsilon_\delta + \varepsilon_\beta - \varepsilon_m - \varepsilon_n)}, \quad (\text{A4})$$

$$+ \sum_{\substack{\delta\alpha\beta \\ pn}} \frac{\langle jp||i\delta\rangle\langle\delta n||\beta\alpha\rangle\langle\alpha\beta||pn\rangle}{(\varepsilon_\delta - \varepsilon_p)(\varepsilon_\alpha + \varepsilon_\beta - \varepsilon_p - \varepsilon_n)}, \quad (\text{A5})$$

$$+ \sum_{\substack{\delta\alpha\beta \\ pn}} \frac{\langle j\delta||ip\rangle\langle\beta\alpha||\delta n\rangle\langle pn||\alpha\beta\rangle}{(\varepsilon_\delta - \varepsilon_p)(\varepsilon_\alpha + \varepsilon_\beta - \varepsilon_p - \varepsilon_n)}. \quad (\text{A6})$$

The A matrix of Reference 12 is:

$$A_{ij} = \delta_{ij}\varepsilon_i + \sum_{k,l} \langle ik||jl\rangle F_{kl}, \quad 21.$$

$$E_{kl} = \sum_{\alpha>\beta,p} K_{\alpha\beta}^{pk} K_{\alpha\beta}^{pl} - \sum_{p<q,x} K_{\alpha l}^{pq} K_{\alpha k}^{pq}. \quad 22.$$

We have thereby calculated the electron propagator consistently through third order.

A comparison with a diagrammatic perturbation expansion of the self-energy (86) makes it further evident that we have really included all terms through third order in our analysis of the electron propagator. In Figure 1 we have displayed the terms A3–A6 as diagrams, using the rules of Brandow (51), which combine the Goldstone

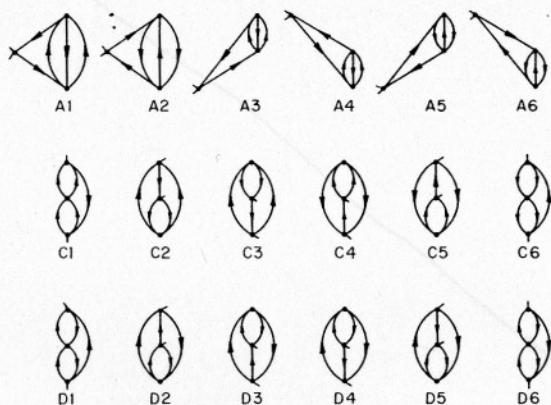


Figure 1 Third-order self-energy diagrams.

diagrams with the antisymmetrized vertices of Hugenholtz. The diagrams labeled A3–A6 are identical to the third order diagrams given by Cederbaum (16), in which dots refer to antisymmetrized vertices. The diagrams A3–A6 were shown by Purvis & Öhrn (49) to be the only missing third-order diagrams that evolve from a theory where the reference state is given by Equation 14. The analysis of Purvis & Öhrn considered $(\mathbf{h}_3|E\hat{I} - \hat{H}|\mathbf{h}_3)$ as two matrices; \mathbf{u} , which contains E and orbital energies (zeroth-order terms), and \mathbf{M} , which contains the two-electron integrals (first-order terms). Making use of the identity $(\mathbf{u} + \mathbf{M})^{-1} = \mathbf{u}^{-1} - \mathbf{u}^{-1}\mathbf{M}(\mathbf{u} + \mathbf{M})^{-1}$ to expand the inverse, Purvis & Öhrn identified the diagrams C1–C6 and D1–D6 of Cederbaum (16) as originating from the $\mathbf{BD}^{-1}\mathbf{C}$ term, while the diagrams A1–A2 were found to arise from the \mathbf{A} matrix previously given in Reference 12. We have thus accounted for all third-order diagrams that arise from an expansion of the self energy. The electron propagator calculation thus needs to use the second-order correlated ground state given in Equation 4 as a reference state and the subspace $\{\mathbf{h}_1, \mathbf{h}_3\}$ given by Equation 3 as the projection manifold in order to be correct through third order.

We have shown how the electron propagator can be obtained correctly through third order. Our development stresses the fact that a complete treatment of the inverse of the \mathbf{D} matrix is needed to guarantee that all desired terms are included. Computational applications have only been carried out so far by using a diagonal approximation to the \mathbf{D} matrix. This situation is unsatisfactory and should be improved. A unitary transformation that brings the \mathbf{D} matrix closer to diagonal form is related to the theory of linear response as discussed by Jørgensen & Purvis (52). By use of this kind of procedure, we would expect to get an approximation to the propagator that would be nearly complete through third order. The energy-shifted denominators that result from evaluating the \mathbf{D} matrix correspond to the result of summing certain classes of diagrams to infinite order, which implies that the electron propagator treatment has the computational advantage of expressing these summations in closed form. In a diagrammatic summation of self-energy diagrams, one has to account explicitly for each energy-shifted denominator through each order. We note finally that the side-shifted diagrams given in Figure 1 do not appear in the original third-order theory of Simons & Smith (12) for calculating ionization potentials and electron affinities. These diagrams result from using a more highly correlated wave function than the one considered by Simons & Smith as the reference state.

With this derivation of the needed third-order equation accomplished, let us now turn to a more detailed description of selected results that have been obtained by making use of the propagator approach. Recall that we are limiting the discussion to studies that have treated electron correlation effects in an *ab initio* manner. The anions that we have chosen to discuss in some detail can be divided into several classes. NH_2^- , OH^- , SH^- , BeH^- , and MgH^- are hydrides whose parents have a half-filled orbital to which the "extra" electron is added. CN^- , BO^- , and NO_2^- are ions whose parents also have half-filled orbitals. All of the above ions are closed-shell species. Li_2^- and Be_2^- are open-shell ions that are formed by adding an electron either to an antibonding (Li_2^-) or bonding (Be_2^-) molecular orbital of the closed-shell parent. LiF^- , LiCl^- , LiH^- , NaH^- , and BeO^- are each formed by adding an electron

to an essentially nonbonding orbital of the very polar neutral parent. Correlation and relaxation are not very important in these ions because the "extra" electron resides in an orbital that is localized on the "back" end of the electropositive atom where it encounters little dynamic interaction with the other electrons.

SURVEY OF RESULTS

OH^-

In carrying out the calculations on OH^- described here (2), we employed an atomic orbital basis consisting of Slater-type functions whose orbital exponents were taken from the bases of Cade (53) for OH^- , and of Cade & Huo (54) for OH. Information describing our basis as well as the essential results of the SCF calculation on the parent $X^1\Sigma^+\text{OH}^-$ for this basis are given in Table 1. Note that the basis used in this work is not very large.

As shown in Table 2, the vertical detachment energies computed using the basis of Table 1 are within 0.1 eV of the experimental result quoted by Lineberger et al (4). An important observation that should be made here is that the basis given in Table 1 is capable of yielding a very accurate detachment energy. Our results show that the theory of molecular electron affinities and ionization potentials in Reference 12 is capable of yielding the vertical electron detachment energy of $X^1\Sigma^+\text{OH}^-$ to within

Table 1 20-function Hartree-Fock wave function for OH^- *

σ atomic orbitals	1 σ	2 σ	3 σ	π atomic orbitals	1 π
01s (7.0168)	0.9721	-0.1645	0.1213	02p (2.0624)	0.5857
02s (2.8646)	0.1268	0.8711	-0.0336	02p' (3.7529)	0.1949
02p (2.1172)	-0.0349	0.0490	0.3761	02p'' (0.7128)	0.3246
01s' (12.3850)	0.0961	0.0081	-0.0111	03d (1.2500)	0.0133
02s' (1.5729)	0.0141	0.3714	-0.3687	H2p (0.9250)	0.0958
02p' (1.0227)	0.0067	-0.0065	0.2047	—	—
02p'' (3.7596)	-0.0053	0.0074	0.1777	—	—
H1s (1.1986)	-0.0027	0.1507	0.4723	—	—
H2s (2.3003)	-0.1816	-0.3336	-0.1403	—	—
H1s' (2.4385)	-0.0014	0.0494	0.0024	—	—

* $R = 1.781$ au, $E = -75.3801$ au, $\epsilon_{1\sigma} = -20.22091$, $\epsilon_{2\sigma} = -0.94178$, $\epsilon_{3\sigma} = -0.27867$, $\epsilon_{1\pi} = -0.12616$.

Table 2 Summary of detachment energies for OH^-

Detachment energy (eV)	Source
1.773	EOM (2)
1.825 ± 0.002	Hotop, Patterson, Lineberger (4)
1.83	Branscomb (3)

0.1 eV. It has also been demonstrated that a highly accurate description of the core orbital of OH^- is not essential to an accurate calculation of the ${}^2\Pi_i$ valence electron detachment energy. Finally, an investigation of the roles of orbital relaxation and correlation-energy change in determining the ion-molecule energy difference has led to the conclusion (2) that both of these effects must be treated properly in any study of negative molecular ions unless one knows that the "extra" electron is essentially uncorrelated (perhaps by spatial localization) with the other electrons. As discussed in a later section on LiF^- , LiCl^- , LiH^- , NaH^- , and BeO^- , such is the case for the family of anions formed by adding an electron to a highly polar, closed-shell molecule.

BeH^-

An initial basis set for the closed-shell (${}^1\Sigma^+$) BeH^- , consisting of 20 Slater-type orbitals (STOs), was adapted from the optimized BeH basis set reported by Cade & Huo (54). To accommodate the extra electron correlation, $2p_\pi$ functions and diffuse s and $2p_\sigma$ functions were added to the "sigma only" BeH basis set to replace functions contributing nominally to the description of the occupied BeH molecular orbitals.

The orbital exponents of the four BeH^- STOs in the original basis set having the largest expansion coefficients in the 3σ highest-occupied molecular orbital (HOMO) were optimized at the initially calculated BeH^- equilibrium internuclear distance of 2.660 au. The initial and optimized BeH^- basis sets and expansion coefficients for occupied molecular orbitals are listed in Table 3. Basis functions that were also used in the Cade & Huo BeH basis set have been marked with an asterisk. From this table we observe that optimization of the BeH^- basis set caused dramatic increases in the importance of the diffuse $2s$ Be and $1s$ H basis functions describing the 3σ HOMO.

Table 3 Original and optimized 20 STO basis sets for BeH^- ^a

BeH basis	Orbital	ζ (original)	ζ (optimized)	$C_{1s}^{(\text{orig})}$	$C_{1s}^{(\text{opt})}$	$C_{2s}^{(\text{orig})}$	$C_{2s}^{(\text{opt})}$	$C_{3s}^{(\text{orig})}$	$C_{3s}^{(\text{opt})}$
*	1sBe	2.9448	—	0.84377	0.85361	-0.16987	-0.15081	-0.09822	-0.08297
*	1s'Be	5.7480	—	0.23092	0.22616	-0.00186	-0.01022	-0.01053	-0.01590
—	2sBe	0.4000	0.4250	0.01243	-0.03928	0.01391	-0.09120	0.63441	1.08018
*	2s'Be	0.8925	1.1500	0.07154	0.10249	0.29861	0.39163	0.63860	0.56833
—	2s''Be	1.7238	—	-0.11599	-0.16573	0.12175	-0.02368	0.06845	-0.05475
—	2p _σ Be	0.4000	—	0.01257	-0.01303	0.03299	-0.03817	-0.13953	-0.01752
*	2p _σ 'Be	0.8080	—	0.03336	0.01491	0.03954	-0.01068	-0.11016	-0.28577
*	2p _σ ''Be	1.0460	—	-0.04211	-0.00897	0.12792	0.13322	-0.08124	0.05031
*	2p _π Be	1.5000	—	0.01356	0.00198	0.09628	0.08734	-0.10446	-0.12637
—	2p _π 'Be	0.8080	—	0	0	0	0	0	0
—	2p _π ''Be	1.0460	—	0	0	0	0	0	0
—	2p _π '''Be	1.5000	—	0	0	0	0	0	0
—	1sH	0.4000	0.3000	-0.05489	0.03915	0.05648	0.15939	-0.47443	-0.73778
—	1s'H	1.0000	1.0500	0.01772	-0.02409	0.71242	0.64325	-0.19299	-0.19021
*	2sH	2.5000	—	-0.00019	0.01496	0.01453	-0.01514	0.00898	0.00635
—	2s'H	1.4500	—	0	0	0	0	0	0

^a Original basis set; $R_e = 2.660$ au, $E = -15.12104$ au, $\epsilon_{1\sigma} = -4.51210$ au, $\epsilon_{2\sigma} = -0.28926$ au, $\epsilon_{3\sigma} = -0.02032$ au; $IP = 0.02751$ au. Optimized basis set; $R_e = 2.670$ au, $E = -15.12308$ au, $\epsilon_{1\sigma} = -4.50693$ au, $\epsilon_{2\sigma} = -0.27730$ au, $\epsilon_{3\sigma} = -0.01877$ au, $IP = 0.02913$ au.

Table 4 Energy vs internuclear separation data in au for BeH and BeH⁻, original and optimized basis sets

$R(\text{au})$	$E_{\text{BeH}}^{\text{orig}}$	$E_{\text{BeH}}^{\text{opt}}$	$E_{\text{BeH}^-}^{\text{orig}}$	$E_{\text{BeH}^-}^{\text{opt}}$	$IP_{\text{BeH}}^{\text{orig}}$	$IP_{\text{BeH}^-}^{\text{opt}}$	$-\epsilon_{3a}^{\text{orig}}$	$-\epsilon_{3a}^{\text{opt}}$
2.380	-15.11607	-15.11785	-15.09207	-15.09201	0.02400	0.02584	—	0.01559
2.420	-15.11750	-15.11935	-15.09307	-15.09311	0.02443	0.02624	0.01781	0.01595
2.460	-15.11868	-15.12056	-15.09381	-15.09392	0.02487	0.02664	0.01818	0.01633
2.500	-15.11959	-15.12150	-15.09422	-15.09441	0.02537	0.02709	0.01857	0.01673
2.538	-15.12023	-15.12217	-15.09439	-15.09465	0.02584	0.02752	0.01895	0.01715
2.580	-15.12070	-15.12269	-15.09429	-15.09467	0.02641	0.02802	0.01940	0.01763
2.620	-15.12096	-15.12297	-15.09401	-15.09446	0.02695	0.02851	0.01985	0.01812
2.660	-15.12104	-15.12308	-15.09353	-15.09409	0.02751	0.02899	0.02032	0.01864
2.700	-15.12097	-15.12303	-15.09284	-15.09348	0.02813	0.02955	0.02081	0.01918
2.740	-15.12076	-15.12284	-15.09201	-15.09275	0.02875	0.03009	0.02133	0.01975
2.780	-15.12042	-15.12251	-15.09101	-15.09184	0.02941	0.03067	0.02188	0.02035

In Table 4 we present our calculated BeH and BeH⁻ energies for both the original and optimized basis sets. SCF calculations for $E_{\text{BeH}}(R)$ were executed on the University of Utah Univac 1108 computer by use of a modified version of the Harris DIATOM program. Execution time for each run was approximately 4.50 min. Vertical ionization energies of BeH⁻ and the $IP_{\text{BeH}}(R)$ were calculated by our third-order equations-of-motion program. Execution time for each ionization energy calculation on the Univac 1108 was approximately 25 sec. BeH energies were calculated by adding the vertical ionization energy of BeH⁻ to the BeH⁻ energy,

$$E_{\text{BeH}}(R) = E_{\text{BeH}^-}(R) + IP_{\text{BeH}^-}(R). \quad 23.$$

Introduction of angular correlation into the BeH⁻ basis set, while necessary for a good description of the electron correlation effects associated with negative-ion ionization energy calculations, resulted in total electronic energy values for both BeH and BeH⁻ that were not as good as those obtained from calculations employing a sigma-only HF basis set. To see this we compare the BeH minimum energy of -15.15312 au, determined by the HF calculations of Cade & Huo (54), with our optimized minimum SCF-EOM BeH energy of -15.09446 au.

In Figure 2 the calculated BeH and BeH⁻ potential curves are presented for the original and optimized basis sets. The energy scale shown in this figure is relative energy in au where the zeros of the curves have all been adjusted so that their shapes may be compared. It is evident from these figures that BeH⁻ has a shallower potential and a larger equilibrium internuclear distance than BeH.

The differences in energies ΔE_{BeH^-} , ΔIP_{BeH^-} , and ΔE_{BeH} between the two basis sets are plotted as a function of R in Figure 3. Since orbital exponents were optimized at the initially calculated equilibrium internuclear distance of BeH⁻ to give the best BeH⁻ energy, it is not surprising that E_{BeH} was more sensitive to this basis set optimization than E_{BeH^-} . For both BeH and BeH⁻ the qualitative effect of BeH⁻ basis set optimization was to increase slightly the slope of the potential curves for $R \lesssim R_e$ and to decrease the slope for $R \gtrsim R_e$, with R_e^{BeH} and $R_e^{\text{BeH}^-}$ becoming slightly larger. We can visualize this by considering the effect of subtracting the ΔE curves in Figure 3 from the original basis BeH and BeH⁻ curves in Figure 2.

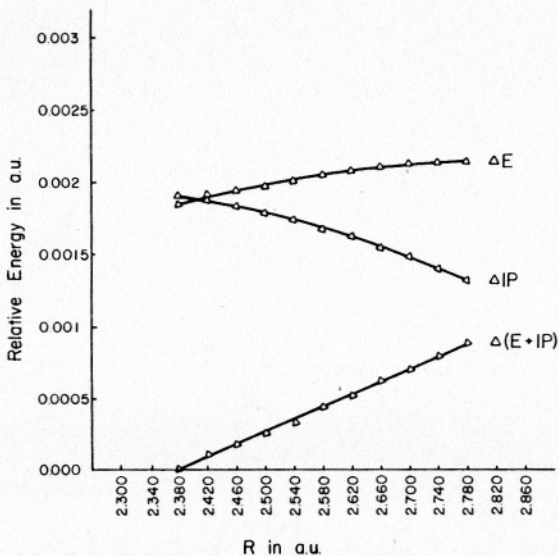
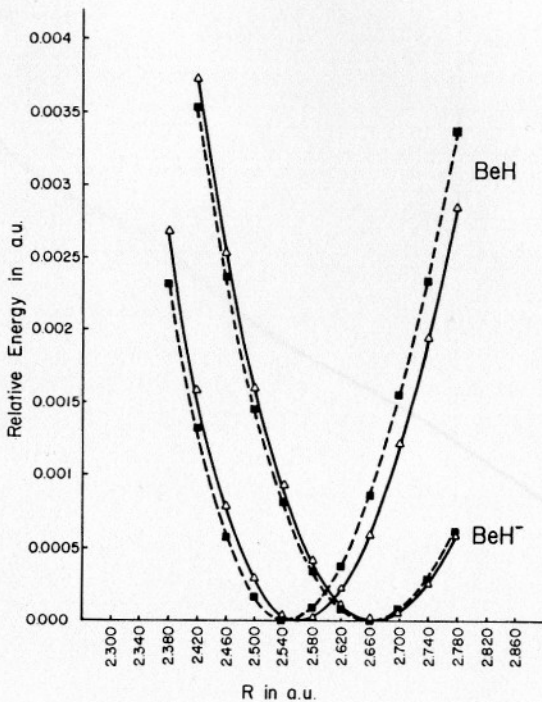


Figure 2 (Top) The original (dashed) and optimized (solid) basis calculation of the BeH^- and BeH energies.

Figure 3 (Bottom) The difference between the original and optimized basis energies of BeH^- (ΔE), IP_{BeH^-} (ΔIP), and BeH [$\Delta(E + IP)$] as functions of R .

Table 5 Calculated and experimental spectroscopic parameters for BeH and BeH⁻

Parameter	Units	BeH ^(exp)	BeH ^(HF)	BeH ^(orig)	BeH ^(op)	BeH ^{-(orig)}	BeH ^{-(op)}	BeH ^{-(exp)}
R_e	au	2.538 ^a	2.528 ^c	2.540	2.560	2.660	2.670	—
k_e	dyne cm ⁻¹ × 10 ⁻¹	2.246 ^{a,b}	2.461 ^c	2.345	2.118	1.903	1.753	—
ν_e	cm ⁻¹	2058.6 ^a	2154.6 ^{a,b}	2103.2 ^b	1998.6 ^b	1894.9 ^b	1818.5 ^b	—
D_e	eV	(2.33) ^{a,b}	2.18 ^c	—	—	2.15 ^e	2.20 ^{d,e}	—
$E_{A_{BeH}}$ (R_e^{BeH})	eV	—	—	0.7031	0.7560 ^d	—	—	—
IP_{BeH} (R_e^{BeH})	eV	—	—	—	—	0.7485	0.7926 ^d	—
IP_{BeH} (thermo)	eV	—	—	—	—	0.7253	0.7727 ^d	0.74 ^a

^a Herzberg (55).^b Gaydon (56), reports 2.3 eV with an uncertainty of ±0.3 eV.^c Cade & Huo (54).^d Results obtained from SCF and EOM calculations at R values not reported in Table 2 of Reference 21.^e Calculated from Cade & Huo HF D_e^{BeH} of 2.18 eV.^f Calculated from Herzberg's D_e^{BeH} of 2.33 eV.^g Feldmann (57), photodetachment energy value corrected for zero-point vibrational energy difference by Equation 19.^h Calculated from k_e or ν_e assuming $\nu_e = 1/2\pi c \sqrt{k_e/\mu}$.

Our calculated spectroscopic parameters for BeH and BeH⁻ are presented in Table 5. Hartree-Fock values and experimental values have been included in this table for comparison with our theoretical results.

Dissociation energies for BeH⁻ were calculated according to the procedure depicted in Figure 4, from which the following can be written:

$$D_e^{BeH^-} = D_e^{BeH} + \Delta D_e, \quad 24.$$

$$\Delta D_e = IP_{BeH} - (R_e^{BeH}) + E_{BeH} - (R_e^{BeH}) - E_{BeH^-} - (R_e^{BeH^-}) - EA_H. \quad 25.$$

Ab initio approximations to $D_e^{BeH^-}$ were obtained using the HF value for D_e^{BeH} of 2.18 eV reported by Cade & Huo. Semi-empirical BeH⁻ dissociation energy results were calculated using Herzberg's BeH dissociation energy (55) of 2.33 eV. Referring to the $D_e^{BeH^-}$ values in Table 5, we can see that the ion-molecule dissociation energy difference ΔD_e is small, and that it changes sign with basis set optimization. Herzberg and, more recently, Gaydon (56) both note the large uncertainty in experimental D_e^{BeH} values. Gaydon reports for D_e^{BeH} 2.3 ± 0.3 eV, an uncertainty that is, of course, much larger than our calculated ΔD_e value. We must therefore assume that a corresponding uncertainty is introduced into our semi-empirical calculations of the negative-ion dissociation energy.

Approximate vibrational force constants and fundamental vibrational frequencies for the BeH and BeH⁻ systems were obtained by fitting a least squares quadratic polynomial to each potential energy curve. Agreement of these calculations with the experimental BeH values was quite good. For the original basis set, $\nu_e^{(calc)} - \nu_e^{(exp)}$ was +44.6 cm⁻¹, a +2.17% deviation, and for the optimized basis set the deviation was -60 cm⁻¹ or -2.91%. For comparison, the value for ν_e^{BeH} reported by Cade & Huo deviated from the experimental value by +96 cm⁻¹ or +4.66%. It is reasonable to assume that our calculated fundamental vibrational frequencies for BeH⁻

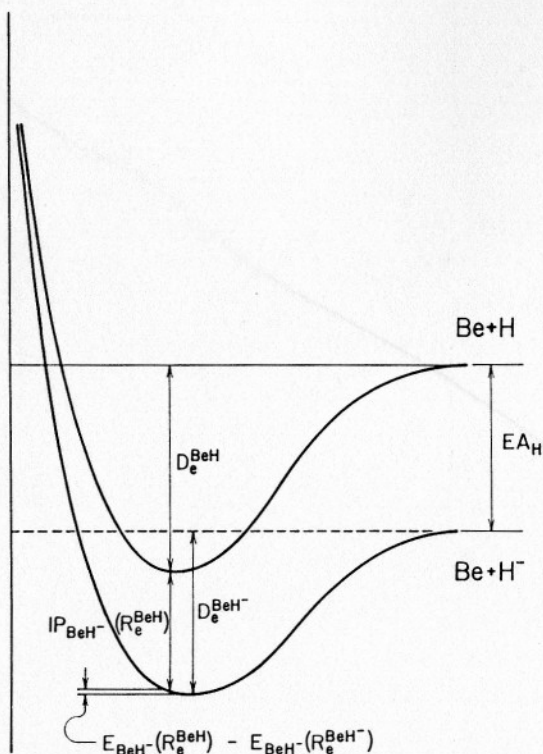


Figure 4 The potential curves of BeH^- and BeH as functions of R .

are at least this accurate. These results for BeH^- should prove extremely useful to experimentalists in the rapidly developing area of negative-ion spectroscopy. The smaller vibrational force constant and the correspondingly lower vibrational frequency for BeH^- as compared to BeH are expected from the relative shapes of their potential energy curves as shown in Figure 2. The fundamental vibrational frequencies for both the negative ion and the neutral molecule decrease with basis set optimization. This trend follows from the widening of the optimized potential wells of the two species described earlier.

The thermodynamic ionization energy of BeH^- was calculated using the relationship:

$$IP_{\text{BeH}^-}(\text{thermo}) = E_{\text{BeH}}(R_e^{\text{BeH}}) - E_{\text{BeH}^-}(R_e^{\text{BeH}^-}), \quad 26.$$

in which $E_{\text{BeH}}(R_e^{\text{BeH}})$ was determined indirectly from our EOM results and the BeH^- energies of the SCF calculation. Vertical ionization energies of BeH^- and vertical electron affinities of BeH were calculated directly from our EOM theory. The threshold photodetachment energy for BeH^- , $\Delta E_{\text{BeH}^-}^{hv}(v^{\text{BeH}} = 0 \rightarrow v^{\text{BeH}} = 0)$, re-

cently determined by Feldmann (57), is related to IP_{BeH^-} -(thermo) by the following equation:

$$IP_{\text{BeH}^-}(\text{thermo}) = \Delta E_{\text{BeH}^-}^{\text{hv}}(0, 0) - h/2(\nu_e^{\text{BeH}} - \nu_e^{\text{BeH}^-}). \quad 27.$$

The second term in Equation 27, which gives the difference in zero-point vibrational energies between BeH and BeH^- , takes into account the fact that the photodetachment energy is the energy difference between zero-point vibrational levels of the negative ion and the neutral, rather than the difference between their potential minima. Calculation of this zero-point vibrational frequency correction gives -0.0129 eV and -0.0111 eV for the original and optimized basis set data respectively. In reporting Feldmann's value for IP_{BeH^-} -(thermo) of 0.74 eV in Table 5, we have thus subtracted 0.01 eV from the BeH^- photodetachment energy value of 0.75 eV. Calculated thermodynamic ionization potentials for BeH^- deviate from the experimental value by $(-0.01 \text{ eV}, -14\%)^{\text{(orig)}}$, $(+0.03 \text{ eV}, +4.1\%)^{\text{(opt)}}$. Vertical ionization energies and electron affinities differ no more than 7% from the experimental thermodynamic value. These results indicate that for reasonable approximations to the thermodynamic ionization energy of BeH^- , our vertical EOM ionization energy calculations at R_e^{BeH} and $R_e^{\text{BeH}^-}$ are quite good.

Our SCF calculations on the $^1\Sigma^+$ BeH^- molecular ion and our third-order EOM ($\text{BeH}^- \rightarrow \text{BeH}$) ionization energy calculations are capable of producing ab initio results for R_e^{BeH} , ν_e^{BeH} , and IP_{BeH^-} -(thermo) in excellent agreement with experiment. These theoretical methods are also capable of yielding new information about BeH^- , such as $R_e^{\text{BeH}^-}$, $\nu_e^{\text{BeH}^-}$, that should be of great value to current experimental efforts in negative ion spectroscopy. Comparisons of the occupied MOs of BeH, BeH^- , and BH make it possible to better understand the influences of electronic and nuclear charge changes in the bonding of these systems.

Our studies of basis set optimization in BeH^- show that good approximations to ion and neutral potential curves, ionization energies, and spectroscopic parameters may be obtained with a carefully chosen nonoptimized basis set. The small differences between $IP_{\text{BeH}^-}(R_e^{\text{BeH}^-})$, $IP_{\text{BeH}^-} - (R_e^{\text{BeH}})$, and IP_{BeH^-} -(thermo) indicate threshold photodetachment energies and thermodynamic ionization potentials can be predicted to within ± 0.05 eV by single EOM vertical ionization energy calculations near the minima of the ion or neutral potential wells.

The EOM-Koopmans' theorem correlation we have observed in our BeH^- and BH ionization energy calculations suggests that we may be able to account for orbital reorganization and electron correlation effects at many internuclear distances by calculating the EOM correction to Koopmans' theorem ionization energy at a single internuclear distance. We feel that the generality of this effect and its theoretical implications are worthy of much more extensive study.

CN^- and BO^-

The starting point for the construction of the double zeta basis sets used in these calculations was Roetti & Clementi's excellent set (58) of double zeta functions for the component atoms. To better describe the charge distribution in the resultant negative molecular ions, the orbital exponents of the functions with large expansion

coefficients in the highest occupied molecular orbital (HOMO) of CN^- and of BO^- were varied to maximize the ionization energies. The greatest changes in each case were produced by modifying the exponents of the $2s$ and $2p\sigma$ functions on the less electronegative atom in the ion.

Since little is known about the geometry of BO^- , its basis set was optimized at $R = 2.278$ bohr, which corresponds to the equilibrium separation of the neutral BO molecule. The total energy before optimization was -99.55 hartree and the corresponding $X^1\Sigma^+ \rightarrow X^2\Sigma^+$ ionization potential was 2.16 eV. The final basis gave a slightly lower SCF energy, -99.554 hartree, and a vertical ionization potential of 2.81 eV.

The CN^- basis set optimizations were performed at $R = 2.2$ bohr, the internuclear separation corresponding to the lowest energy found after doing a few preliminary SCF calculations on CN^- with the starting basis. The initial energy at 2.2 bohr was -92.2634 hartree, and the vertical ionization energy for the starting basis was 3.04 eV. After optimization of $2s$ and $2p\sigma$ functions on carbon and $2s$ functions on nitrogen, the total energy was -92.2645 hartree and the $X^1\Sigma^+ \rightarrow X^2\Sigma^+$ vertical ionization energy was 3.69 eV. The diffuse $2p\pi$ function on nitrogen was varied slightly in an attempt to obtain a reasonable $^1\Sigma \rightarrow ^2\pi$ ionization potential. However, the $^2\pi$ state of CN is not expected to be well described in our basis since the optimization of the pi functions was not extensive. The final optimized CN^- and BO^- basis sets shown in Table 6 were used to compute ion-molecule energy differences at several internuclear separations; these differences were added to the total SCF energies at corresponding R values of the negative ions to generate SCF-level potential curves for BO and CN.

Examination of the ground-state potential curves for BO, BO^- , CN, and CN^- allows us to determine the adiabatic electron affinities of BO and CN, which we

Table 6 Basis sets (STOs) for CN^- and BO^-

CN ⁻						BO ⁻					
σ orbitals			π orbitals			σ orbitals			π orbitals		
center	n1	ζ	center	n1	ζ	center	n1	ζ	center	n1	ζ
C	1s	5.1231	C	2p	1.2566	B	1s	4.2493	B	2p	0.9500
C	1s	7.5223	C	2p	2.7304	B	1s	6.5666	B	2p	2.2173
C	2s	0.9750	N	2p	1.3380	B	2s	0.8250	O	2p	1.5200
C	2s	1.9400	N	2p	3.2493	B	2s	1.6500	O	2p	3.6944
C	2p	1.2566				B	2p	0.8500			
C	2p	2.8700				B	2p	2.2173			
N	1s	5.9864				O	1s	6.8377			
N	1s	8.4960				O	1s	9.4663			
N	2s	2.3500				O	2s	2.8200			
N	2s	1.3750				O	2s	1.6754			
N	2p	1.4992				O	2p	1.6586			
N	2p	3.2493				O	2p	3.6944			

can compare with existing experimental data. Our predicted electron affinity for BO, 2.79 ± 0.2 eV, is within the range of experimental estimates (59) that vary from 2.4 eV to 3.1 ± 0.1 eV. Experimental studies of CN have yielded more precise results. Chupka et al (60) have reported an electron affinity of 3.82 ± 0.02 eV that was obtained from photodissociation measurements of HCN. Our calculated electron affinity, 3.70 ± 0.2 eV, is in good agreement with this value.

The results of our EOM calculations and Koopmans' theorem estimates for vertical ionization potentials of CN^- and BO^- are shown in Table 7 for selected internuclear separations. The Koopmans' theorem values deviate considerably from EOM results for the ${}^1\Sigma^+ \rightarrow {}^2\Sigma^+$ ionization of CN^- , less so for the ${}^1\Sigma^+ \rightarrow {}^2\Sigma^+$ BO^- ionization, and are actually very close to EOM results for the ${}^1\Sigma^+ \rightarrow {}^2\pi$ ionization of CN^- .

The large difference between Koopmans' theorem and the EOM result for the ${}^1\Sigma^+ \rightarrow {}^2\Sigma^+$ ionization of CN^- indicates that orbital relaxation and electron correlation effects are important in the process of removing an electron from the 5σ orbital of CN^- . Analogously, relaxation and correlation effects appear to be less important in the ionization of BO^- .

We have used the EOM method to study the stability of BO^- and CN^- and to investigate the nature of the highest occupied molecular orbital in each of these species. Our calculations show a ${}^1\Sigma^+ \rightarrow {}^2\Sigma^+$ ionization energy of 2.88 eV for BO^- at 3.35 bohr, the equilibrium internuclear separation (R_e) of the ion, and an ionization potential of 2.81 eV at the R_e of BO, 2.278 bohr. The resulting adiabatic electron affinity of BO, 2.79 eV, falls within the range of experimental values (59) obtained for this quantity. The EOM ionization potential (${}^1\Sigma^+ \rightarrow {}^2\Sigma^+$) of CN^- was found to be 3.69 eV at $R = 2.25$ bohr, the equilibrium separation of both the ion and the molecule. This result is very close to the experimental electron affinity of CN determined from photodissociation experiments (60).

In each of these ions, the electron is ionized out of a nonbonding 5σ molecular orbital consisting mainly of diffuse $2s$ and $2p_z$ functions on the less electronegative

Table 7 Selected CN^- and BO^- ionization potentials

R (au)	CN^-				BO^-		
	${}^1\Sigma^+ \rightarrow {}^2\Sigma^+$		${}^1\Sigma^+ \rightarrow {}^2\Pi$		${}^1\Sigma^+ \rightarrow {}^2\Sigma^+$		
	IP(eV)	$-\epsilon_{5\sigma}$ (eV)	IP(eV)	$-\epsilon_{1\pi}$ (eV)	R (au)	IP(eV)	$-\epsilon_{5\sigma}$ (eV)
2.75	3.74	4.62	3.60	3.53	2.80	3.10	3.56
2.70	3.74	4.70	3.76	3.70	3.35 ^a	2.88	3.23
2.35 ^c	3.71	5.14	4.93	5.01	2.278 ^b	2.81	3.14
2.30	3.70	5.18	5.11	5.21	2.20	2.72	3.04
2.25 ^{a,b}	3.69	5.21	5.29	5.43			
2.00	3.65	5.23	6.28	6.60			

^a R_e of the ion.

^b R_e of ${}^2\Sigma^+$ state of the neutral.

^c R_e of ${}^2\Pi$ state of the neutral.

atom in the ion. For CN^- , there is also some contribution from the diffuse $2p_\sigma$ nitrogen function. The character of the 5σ orbital in the isoelectronic sequence, N_2 , CN^- , CO , BO^- , changes in a regular fashion; the electron density in the 5σ orbital becomes more polarized toward the less electronegative atom as the electronegativity difference between the constituent atoms increases.

The $^2\Sigma^+$ and $^2\pi$ states of CN were found to cross at about 2.75 bohr, whereas the Koopmans' theorem ionization energies predict the crossing at 2.35 bohr. The situation in the region from 2.35 to 2.75 bohr is analogous to the observed energy-ordering of N_2 orbitals and N_2^+ states, and is interpreted in terms of the larger correlation-energy correction to Koopmans' theorem for ionization from the 5σ orbital of CN^- rather than from the 1π orbital.

Li_2

The EOM method discussed in Reference 12 requires as input the results of an SCF calculation on the closed-shell parent, Li_2 . These SCF results were obtained using the Harris DIATOM program, which is run on the University of Utah Univac 1108 computer. The basis set was formed by starting with a basis for the lithium atom reported by Clementi (61). To this set of Slater-type functions we added one full set of diffuse p functions and another set of p_π -type functions. The basis was then optimized to give the maximum value for the electron affinity of Li_2 . Based upon our experience with other molecules, we find that this procedure of optimization leads to the best balanced description of the parent, Li_2 , and the anion, Li_2^- .

During the optimization the need for a more diffuse $2s$ function became apparent. The first three $2p$ functions on each lithium atom were optimized together as a set. After attempting to optimize the p_σ and s orbitals to yield the maximum value for the electron affinity, we added another set of diffuse p_π functions whose exponents were then optimized. All optimization was performed at 5.3 bohrs, which is near our computed equilibrium bond length of Li_2 . The resulting basis set is shown in Table 8. The results of this optimization gave a vertical electron affinity of 0.80 eV for Li_2 at $R = 5.3$ bohr (94).

The spectroscopic parameters of Li_2 and Li_2^- were determined by least squares fitting a parabola to the bottom of the respective potential curves. The results of this calculation are given in Table 9.

The dissociation energy of Li_2^- was calculated from Equation 28:

$$D_0(\text{Li}_2^-) = D_0(\text{Li}_2) + \text{E.A.}(\text{Li}_2, \text{thermo}) - \text{E.A.}_{\text{Li}}, \quad 28.$$

where $D_0(\text{Li}_2)$ is the chemical dissociation energy of Li_2 ; $D_0(\text{Li}_2^-)$ is the chemical dissociation energy of Li_2^- ; $\text{E.A.}(\text{Li}_2, \text{thermo})$ is the thermodynamic electron affinity; and E.A._{Li} is the electron affinity of the lithium atom. The dissociation energy of Li_2 was obtained from the experimental determination of Velasco et al (65). The electron affinity for atomic Li has also been determined experimentally (66). The thermodynamic electron affinity appearing in Equation 28 was obtained from the calculated Li_2 and Li_2^- potential curves by making harmonic zero-point energy corrections to the difference in the minimum electronic energies. This procedure results in a

Table 8 The optimized 20 STO basis set for Li_2 and the coefficients for the occupied orbitals at 5.3 bohrs^a; $E = -14.86325^b$

Orbital	ζ	$C_{1\sigma}$	$C_{2\sigma}$	$C_{3\sigma}$
1sLi	2.4739	0.63248	0.63664	-0.07663
1sLi'	2.4739	0.63687	-0.63224	-0.07663
1s'Li	4.6925	0.07906	0.07974	-0.02727
1s'Li'	4.6925	0.07968	-0.07919	-0.02727
2sLi	0.3523	0.00004	-0.00752	0.19206
2sLi'	0.3523	-0.00001	0.00752	0.19208
2s'Li	1.0287	-0.00016	-0.00232	0.56164
2s'Li'	1.0287	-0.00017	0.00232	0.56164
2s''Li	1.6350	0.00501	0.00573	-0.26926
2s''Li'	1.6350	0.00505	-0.00570	-0.26926
2p _σ Li	0.4066	-0.00054	-0.00352	0.18068
2p _σ Li'	0.4066	0.00057	-0.00352	-0.18068
2p _π Li	0.4066	0	0	0
2p _π Li'	0.4066	0	0	0
2p _{π'} Li	0.6449	0	0	0
2p _{π'} Li'	0.6449	0	0	0

^a The asymmetry in the coefficients is due to convergence criteria problems.

^b This SCF energy is not as good as that reported by Das (62).

Table 9 Molecular properties for Li_2 and Li_2^-

Parameter	Unit	$\text{Li}_2^-(\text{calc})$	$\text{Li}_2^-(\text{exp})$	$\text{Li}_2^-(\text{calc})$
R_e	au	5.29	5.051 ^a	6.3
K_e	$\text{dyne cm}^{-1} \times 10^{-4}$	2.112	—	0.7849
v_e	cm^{-1}	319.7	351.43 ^a	194.9
D_e	eV	—	1.026 ± 0.006^b	1.31
E.A.(vert)	eV	0.8	—	—
IP	eV	—	5.15 eV ^c	1.06
E.A.(thermo)	eV	0.9	4.94 eV ^d	—

^a Herzberg (63).

^b Velasco et al (65).

^c P. J. Foster, R. E. Leckenby, E. J. Robbins. 1969. *J. Phys. B* 2:478. (Isotopic Li_2).

^d A. M. Emel'yanov, V. A. Peredvignina, L. N. Gorokhov. 1971. *High Temp.* 9:164. (Isotopic Li_2).

predicted thermodynamic electron affinity of 0.9 eV and a calculated $D_0(\text{Li}_2^-)$ of 1.31 eV.

The ground state of Li_2^- has been reported by Linnett et al (67) to be $^2\Pi_u$. In the Linnett calculations, the $^2\Pi_u$ state is more stable than the $^2\Sigma_u^+$ state by 0.016 hartree (0.44 eV). We find in this work that the $^2\Sigma_u^+$ state is more stable than the $^2\Pi_u$ by 0.6 eV at 5.3 bohrs, based upon a difference of optimized vertical electron affinities for the two states.

By using the potential curves discussed above, together with the calculated vibrational frequency of Li_2^- and the measured frequency of Li_2 , we determined the thermodynamic electron affinity of Li_2 to be 0.9 eV. This is substantially larger than the 0.27 eV reported by Linnett (67) for the ${}^2\Pi_u$ state of Li_2^- . The calculation of the vertical photodetachment energy of Li_2^- can also be achieved from the above-mentioned potential energy curves. For this quantity, we obtain a value of 1.06 eV.

It is very interesting to make use of the results of the present calculations to compare the bonding and spectroscopic parameters of Li_2^+ and Li_2^- , both of which have a bond order of one half. Calculations on Li_2^+ give a fundamental frequency (68) of 254.7 cm^{-1} , which is not very different from the fundamental frequency of Li_2^- determined in this work (195.9 cm^{-1}). Several values of the dissociation energy of Li_2^+ have been tabulated by Wahl et al (68). One of the more recent values (1.31 eV) (69) is identical to our computed dissociation energy of Li_2^- .

By comparing these spectroscopic parameters for Li_2^+ and Li_2^- to those of the neutral molecule, we see that Li_2 has a stronger bond (larger ω_e , shorter R_e) than the ions; however, both of the ions are more stable (larger D_0) than the neutral Li_2 . The positive and negative ions have very similar bond lengths (both ~ 6 bohrs) that are 1 bohr longer than that of the neutral. This is in line with the difference in bond order between the neutral Li_2 and its ions. The fact that the ions have a larger dissociation energy may be related to the long-range ion-atom interaction. A set of minimal-basis valence bond calculations (64) on Li_2 , Li_2^+ , and Li_2^- provides data that tend to support our findings. In Reference 64 the resulting dissociation energies of Li_2 , Li_2^+ , and Li_2^- are 0.76 eV, 1.06 eV, and 0.92 eV, respectively.

Previous calculations (2, 20–25) have shown how well the EOM method has succeeded in obtaining electron affinities of molecules in cases where experimentally determined values were known. This indicates that by applying the EOM method valuable predictions can be made. From this work we obtain a prediction that the ${}^2\Sigma_u^+$ ground state of Li_2^- is stable with respect to dissociation and electron loss. We find that the ground state of Li_2^- should be as stable to dissociation as Li_2^+ . The overlap of the $r = 0$ Li_2 and Li_2^- vibrational wave functions is so small that we conclude that the vertical electron affinity and photodetachment measurements should give significantly different values for this system. Furthermore, we have found the $\text{Li}_2-\text{Li}_2^-$ system to be very interesting because the large change in internuclear separation in going from Li_2 to Li_2^- is accompanied by a decrease in vibrational frequency and an increase in dissociation energy. Such a seemingly anomalous situation also occurs in going from Li_2 to Li_2^+ .

LiF⁻, LiCl⁻, LiH⁻, NaH⁻, BeO⁻

In a communication (70) we made theoretical predictions of stable negative ions of LiH and NaH. Later, we described in a full paper (25) the research that led us to the prediction of the existence of these stable anions. We also presented results that showed that the BeO^- and LiF^- anions are stable with respect to dissociation and autodetachment. We reexamined the HF^- anion, and concluded that it is unstable at the equilibrium configuration of HF. In an extension of this work, Jordan (90) has investigated the possible existence of H_2O^- , HCN^- , and $(\text{HF})_2^-$,

all of which he finds to be unstable with respect to electron detachment near the equilibrium geometry of the parent.

It has been demonstrated by several researchers (71–76) that an electron in the field of a fixed, finite dipole greater than 1.625 Debye possesses an infinity of bound states. Although LiH, NaH, BeO, and LiF all have dipole moments in excess of this value, stable negative ions of these species have not been detected experimentally or predicted from *ab initio* calculations prior to our investigations.

A stable negative ion of LiCl has been detected by Carlsten, Peterson & Lineberger (27), and the Hartree-Fock predictions on LiCl⁻ of Jordan & Luken (77, 80) are in good agreement with the experimental results. In view of the nonbonding nature of the orbital occupied by the extra electron demonstrated by this theoretical study, inclusion of electron correlation would be expected to result in only a small correction to the description of the binding of an electron to LiCl. That this expectation is confirmed by the good agreement with the Hartree-Fock method in describing the binding of an electron to LiCl suggests the possibility of similar results with other highly polar molecules.

The experimental and theoretical studies on LiCl⁻ indicated that the simple, fixed, finite dipole model provides an inadequate description of the binding of an electron to LiCl. One of the motivations of our work is to provide a more extensive evaluation of the validity of the dipole model.

The most essential aspect of our investigation of the binding of electrons to polar molecules is the choice of basis sets in which diffuse functions are added to the electropositive atom to permit the "extra" electron to "attach" itself to the positive end of the polar parent molecule. Most of the calculations in the present paper employ Slater-type orbitals (STOs); the unnormalized STOs are functions of the type $r^{n-1}e^{-\zeta r}$, where n is the principal quantum number and ζ the orbital exponent. In Table 10 we list the STO basis sets employed in our calculations.

In Table 11 the KT (Koopmans' theorem) and EOM electron affinities are presented for the equilibrium bond length of the parent neutral. Perhaps the most striking observation to be drawn from these data is that orbital relaxation and correlation corrections to the EAs are small, in marked contrast to the situation encountered with covalent molecules such as OH, O₂, and NO, for which orbital relaxation and correlation corrections to the electron affinities are typically an eV or more. The small correlation and relaxation energy changes that occur with the formation of the ions from the neutrals are in accord with a description in which the "extra" electron resides in a region of space that is essentially unoccupied by other electrons. Apparently, the orbital picture provides a good first approximation to the binding of electrons to highly polar molecules.

The second unoccupied σ orbital of LiCl was found to have a negative energy (~ -0.007 eV) when very diffuse $3s$ and $3p_{\sigma}$ functions were placed on the lithium. A similar result is observed for LiF, and probably would be observed for NaH, BeO, and LiH if sufficiently diffuse functions of the appropriate symmetry were included in the basis sets. However one should not attach much physical significance to such weakly bound states, since they would probably become unbound if corrections to the Born-Oppenheimer approximation were included. It is possible that

Table 10 STO basis set for LiH, LiF, NaH, HF, and BeO^a

LiH		LiF		NaH		BeO	
1s _σ Li	(4.6990)	1s _σ Li	(4.6925)	1s _σ Na	(11.1543)	1s _σ Be	(6.4072)
1s' _σ Li	(2.5212)	1s' _σ Li	(2.4739)	2s _σ Na	(2.0006)	1s' _σ Be	(3.5297)
*2s _σ Li	(1.2000)	2s _σ Li	(1.6350)	2p _σ Na	(4.1786)	2s _σ Be	(1.1956)
*2s' _σ Li	(0.7972)	*2s' _σ Li	(1.0287)	2p' _σ Na	(2.2798)	*2s' _σ Be	(0.8557)
*2s'' _σ Li	(0.6000)	*2s'' _σ Li	(0.5352)	3s _σ Na	(6.2601)	*2s'' _σ Be	(0.4677)
*2s''' _σ Li	(0.3000)	*2s''' _σ Li	(0.3223)	3s' _σ Na	(0.9106)	2p _σ Be	(2.0717)
2p _σ Li	(2.7500)	*2p _σ Li	(0.4066)	3s'' _σ Na	(0.4000)	*2p _σ Be	(0.8557)
2p' _σ Li	(1.2000)	2p' _σ Li	(0.4066)	*3s''' _σ Na	(0.2000)	*2p' _σ Be	(0.4677)
2p'' _σ Li	(0.7369)	1s _σ F	(14.1095)	3p _σ Na	(1.2631)	2p _π Be	(1.0846)
2p''' _σ Li	(0.6000)	1s' _σ F	(7.9437)	3p' _σ Na	(0.7108)	1s _σ O	(7.6092)
*2p _σ ''''Li	(0.3000)	2s _σ F	(3.2563)	*3p'' _σ Na	(0.4000)	2s _σ O	(3.1394)
2p _π Li	(0.7369)	2s' _σ F	(1.9346)	3p''' _σ Na	(0.1500)	2s' _σ O	(0.8792)
2p' _π Li	(0.3500)	2p _σ F	(4.2784)	2p _π Na	(4.1742)	2p _σ O	(3.4198)
2s _σ H	(1.5657)	2p' _σ F	(2.3732)	2p' _π Na	(2.2828)	2p' _σ O	(1.7405)
1s' _σ H	(0.8877)	2p'' _σ F	(1.4070)	3p _π Na	(0.9636)	2p'' _σ O	(1.0626)
*2s _σ H	(0.4000)	2p _π F	(2.3291)	1s _σ H	(0.7808)	2p _π O	(3.4198)
2p _σ H	(1.3765)	2p' _π F	(1.3584)	*2s _σ H	(0.4000)	2p' _π O	(1.7405)

^a LiH: $Re = 3.015$ au; $E = -7.9866$ au; LiF: $Re = 2.955$ au; $E = -106.584$ au; NaH: $Re = 3.566$ au; $E = -161.9422$ au; BeO: $Re = 2.51$ au; $E = -89.3432$ au.

Table 11 Equations-of-motion electron affinities and Koopmans' theorem estimates (eV)

	LiH(5.88) ^a	LiF(6.33)	LiCl(7.13)	NaH(6.98)	BeO(7.41)
EOM ^b	0.2986	0.4645	[0.54/0.61]	0.3618	1.7692
-LUMO ^b	0.1997	0.4252	0.48	0.2897	1.4144
Orbital relaxation and correlation corrections ^c	0.0989	0.0393	0.13	0.0721	0.3548

^a The quantities in parenthesis are the dipole moments in Debye. The dipole moment of BeO has not been experimentally determined. The value listed is that calculated by Yoshimine (78). The experimental dipole moments for the other molecules are listed. These values are taken from the tables of R. D. Nelson, D. R. Lide, A. A. Maryott, *Selected Values of Electric Dipole Moments for Molecules in the Gas Phase*, U.S. Dept. Commerce, Natl. Bur. Stand.

^b The LiCl LUMO orbital energy is from Jordan, Herzenberg & Luken (77). An EOM calculation has not been performed on LiCl. The value of 0.54 eV was obtained from a ΔE_{HF} [$\Delta E_{\text{HF}} = E_{\text{HF}}(\text{LiCl}) - E_{\text{HF}}(\text{LiCl}^-)$] calculation, while the value of 0.61 eV is the experimental value of Carlsten, Peterson & Lineberger (27).

^c For LiH, LiF, NaH, and BeO the orbital relaxation and correlation corrections are obtained by subtracting the Koopmans' theorem estimate of the electron affinity from the EOM value. For LiCl the experimental electron affinity is used in place of the EOM value.

molecules with substantially larger dipole moments such as CsCl ($\mu = 10.4$ Debye), could have two stable negative ion states near the equilibrium separation of the parent molecule. Certainly if the dipole moment becomes large enough, the first excited anion state will remain stable even when corrections to the Born-Oppenheimer approximation are included.

Figures 5-8 display the ground state potential energy curves of LiH, LiF, NaH, BeO, and their anions. The potential energy curves of the neutral parent molecules

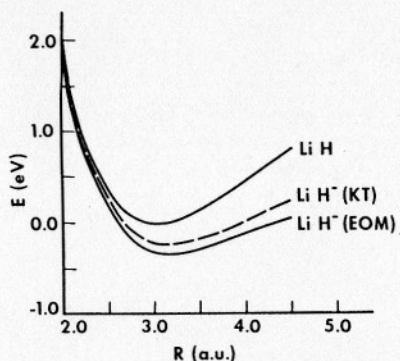


Figure 5 The potential energy curves of LiH and LiH⁻ (obtained from Koopmans' theorem and EOM) as functions of R .

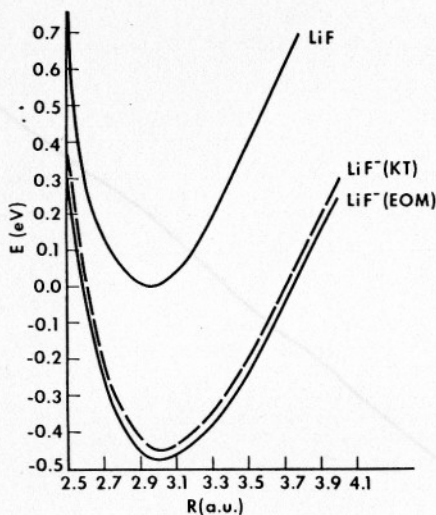


Figure 6 The potential energy curves of LiF and LiF⁻ (obtained from Koopmans' theorem and EOM) as functions of R .

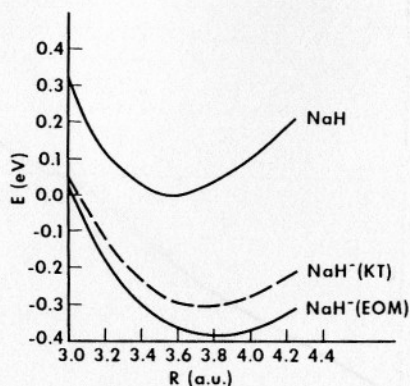


Figure 7 The potential energy curves of NaH and NaH⁻ (obtained from Koopmans' theorem and EOM) as functions of R .

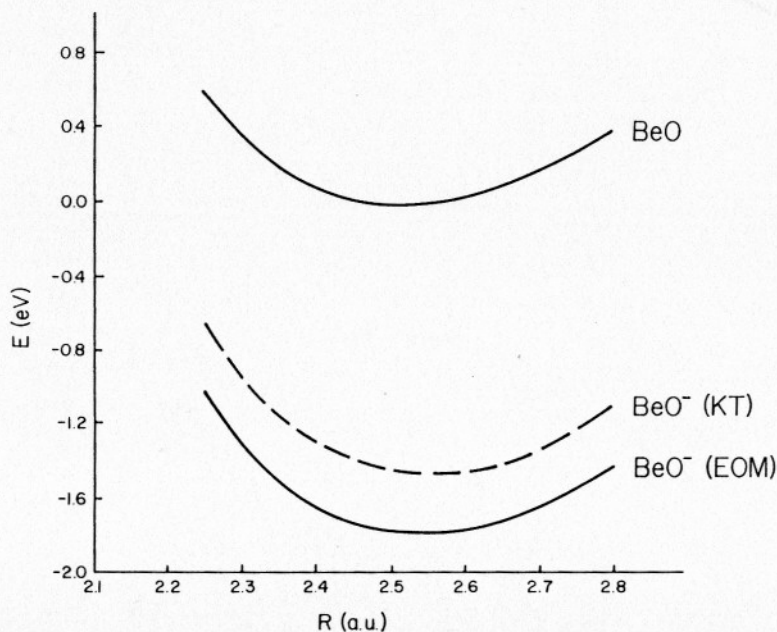


Figure 8 The potential energy curves of BeO and BeO⁻ (obtained from Koopmans' theorem and EOM) as functions of R .

are constructed from experimental data via the Padé approximant procedure (81):

$$U_{\text{PA}}(X) = a_0 X^2 / [1 - a_1 X + (a_1^2 - a_2) X^2], \quad 29.$$

where $X = (R - R_e)/R_e$ and a_0, a_1, a_2 are determined from the spectroscopic constants $\omega_e, \omega_e \chi_e, B_e,$ and α_e as follows:

$$a_0 = \omega_e^2 / 4B_e, \quad 30.$$

$$a_1 = -(\omega_e \alpha_e / 6B_e^2) - 1, \quad 31.$$

$$a_2 = \frac{5}{4} a_1^2 - \left(\frac{2}{3}\right) (\omega_e \chi_e / B_e). \quad 32.$$

The Padé approximant given by Equation 29 provides a particularly good representation of the potential curves of ionic molecules near their equilibrium configurations. For example, for the range of R considered in Figure 5, the potential curve for LiH given by Equation 29 is essentially indistinguishable from the RKR curve and is very close to the potential curve of Docken & Hinze (82) obtained from a configuration interaction calculation. In Table 12 we list the spectroscopic constants $\omega_e, \omega_e \chi_e, \beta_e, \alpha_e,$ and R_e for the molecules being considered.

It is appropriate at this point to compare our calculated electron affinities with those of the fixed finite dipole model. In Figure 9 we have plotted the binding energy of the first three states of an electron in the field of a fixed dipole moment as a function of the dipole moment. Here we have specifically considered the case of a dipole arising from two charges, $+q$ and $-q$, where $q = 1$. For LiH, LiF, LiCl,

Table 12 Experimental spectroscopic constants for the neutral ions, and calculated spectroscopic constants for the anions^a

Parameter	Units	LiH	LiF	LiCl	NaH	BeO
R_e	au	3.015	2.956	3.814	3.566	2.516
ω_e	cm ⁻¹	1405.6	910.3	662	1172.2	1487.3
$\omega_e \chi_e$	cm ⁻¹	23.20	7.929	4.501	19.72	11.83
B_e	cm ⁻¹	7.5131	1.3454	0.625	4.9001	1.6510
α_e	cm ⁻¹	0.2132	0.0201	0.0079	0.1353	0.0190
Parameter	Units	LiH ⁻	LiF ⁻	LiCl ⁻	NaH ⁻	BeO ⁻
R_e	au	3.20	3.00	4.01	3.80	2.54
ΔR_e	Å	0.08	0.02	0.10	0.12	0.01
ω_e^b	cm ⁻¹	1250	840	525	960	1360
% change in ω_e	%	11	8	21	18	8
D_e	eV	1.94	3.02	1.84	1.65	4.86

^a The values of $\omega_e \chi_e$ for LiCl, and the values of α_e for LiF and LiCl are from P. Brumer and M. Karplus. 1973. *J. Chem. Phys.* 58:3903. The rest of the data for the neutral species are from Reference 23.

^b The ω_e are obtained by fitting points on the negative ion curve obtained by subtracting the EOM electron affinity from the potential curve of the neutral parent molecule. The uncertainty in ω_e due to our fitting procedure, is probably $\sim \pm 50$ cm⁻¹.

and NaH q is close to one, so the choice of $q = 1$ introduces only a small error. As was pointed out in Reference 77, one should not attempt to correlate the ground state negative ions of these molecules with the $(0, 0, 0)$ ground state of the dipole model, since this state of the dipole model does not have the correct nodal behavior. There is, however, a qualitative correlation between the ground state negative ions where lithium is the electropositive species and the first excited $(1, 0, 0)$ state of the dipole model. Similarly, for species where sodium is the electropositive species there is a qualitative correlation of the negative ions with the second excited state $(2, 0, 0)$ of the dipole model. This correlation is apparent from Figure 9. These correlations would become much more quantitative if core penetration effects were incorporated in the dipole model. For example, near R_e LiCl is well described as Li^+Cl^- , where the Li^+ has a $(1s)^2$ core. In the negative ion the nonbonding LUMO has a node ~ 0.8 au behind the lithium, while the dipole model, for a dipole moment of 7.2 Debye, locates the node 2.7 au behind the positive center. The ab initio calculations allow lithium $2s$ and $2p$ electrons to penetrate the $(1s)^2$ core and "feel" the $+3$ nuclear charge; this important effect is not accounted for in the dipole model. This is a major source of the discrepancy between the dipole model and the more realistic ab initio calculations.

We know that the ground-state negative ion of BeO should also correlate with the $(1, 0, 0)$ state of the dipole model. The electron affinity of BeO has not been included in Figure 9 since BeO is not a monovalent species. To compare the electron

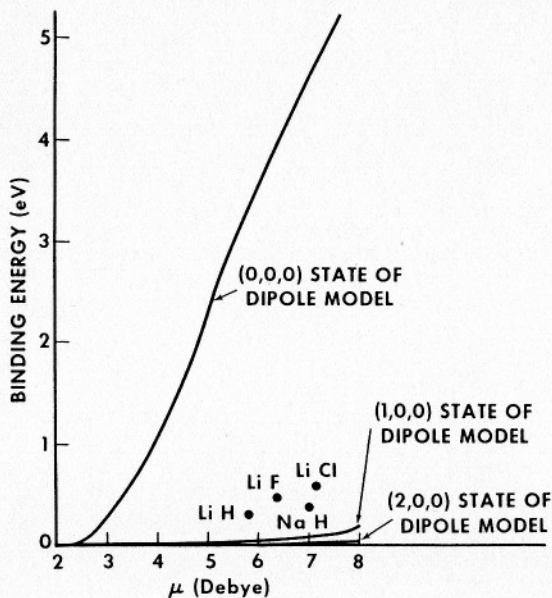


Figure 9 Correlation between dipole moment and electron affinity, and comparison with dipole model.

affinity of BeO with the dipole model predictions, we would have to repeat the calculations for $q \approx 1.5$.

LiH, LiF, LiCl, and NaH all have dipole moments between 5.8 and 7.2 Debye, and all have computed (vertical) electron affinities between 0.3 and 0.6 eV. It would be of interest to determine the electron affinities of molecules with dipole moments in the 3–6 Debye range. For dipole moments ≤ 6 Debye the electron affinities should be ≤ 0.3 eV. These cases will pose special difficulties. The considerations of this work have assumed the validity of the Born-Oppenheimer approximation. As stressed by Garrett (75), one should allow for the fact that the dipole is nonstationary. Anions that are weakly bound under the assumption of the validity of the Born-Oppenheimer approximation may turn out to be unbound when corrections to the Born-Oppenheimer approximation are included.

In this section we have presented calculations on the ground state anions of LiH, LiF, NaH, and BeO. In each case, the extra electron is found to occupy a predominantly nonbonding orbital. This results in small orbital relaxation and correlation corrections, as well as only a small increase of the internuclear separation and a small (10–20%) decrease in ω_e upon formation of the ion. The electron affinities as predicted by the dipole model are found to be in poor agreement with those of our *ab initio* calculations. We attribute this disagreement to the neglect of core penetration in the dipole model.

There are several possible extensions and applications of the work presented in this paper. We intend to report on negative ions of various polar polyatomic molecules in future publications. We are also investigating whether the stable negative ions of ionic molecules may influence the mechanisms of certain chemical reactions. In collisions between an ionic molecule and an atom or molecule with a low ionization potential, an electron-jump mechanism may play a role. For example, an excited cesium atom could lose an electron to LiCl. Furthermore, this would tend to favor a "backside" attack, proceeding through a $\text{Cs}^+(\text{LiCl})^-$ intermediate as opposed to LiClCs. The possibility of formation of Li from the reaction of Li^- with X_2 is particularly interesting. Although alkali-halogen reactions have long been a favorite in studies of collision dynamics, to date the experimental studies have dealt with neutral or positively charged species.

It is hoped that the calculations and suggested new reaction pathways presented in this paper will stimulate experimental investigations of the anions of highly polar molecules.

Other Recent Results

In addition to the investigations that are described in some detail in the preceding parts of this section, studies of numerous other anions have been carried out by ourselves and others since 1968. We have completed preliminary studies of MgH^- , SH^- , NH_2^- , and NO_2^- that tie in with our work on BeH^- , OH^- , and with the works of Schaefer (42), Lineberger (89), and Brauman (88) on NO_2^- , and of Brauman (87) and Hall (87) on NH_2^- . For these systems, our computed vertical detachment energies, together with the experimental and theoretical results of others are shown in Table 13.

Table 13 Computed and experimental vertical detachment energies (eV)^a

Anion	Our D E	Experimental D E	Other theoretical D E
MgH ⁻	0.85	0.8 (57)	—
SH ⁻	2.20	2.32 (83)	2.25 (11)
NH ₂ ⁻	0.42	0.74 (87)	0.30 (41)
NO ₂ ⁻	2.68 (79)	2.8 (88)	3.45 (33)
	2.42 (adiabatic)	2.36 (89) (adiabatic)	

^a Numbers in parentheses designate reference sources.

Quite recently, Jordan (90) has undertaken the study of a number of anions whose neutral parents have very large dipole moments. This is an extension of the work of Jordan and ourselves described in the preceding part of this section. Jordan has predicted the stability and spectroscopic characteristics of the following anions: LiCN⁻, LiNC⁻, Li₂O⁻, (LiH)₂⁻ (92), LiCH₃⁻, LiOH⁻, and LiN⁻. He has also carried out some very nice work, in collaboration with Burrow (91) on metastable organic molecular anions (ethylene, butadiene, substituted benzenes). Jordan & Simons (93) have found the lowest ²Σ_g state of Be₂⁻ to be stable with respect to dissociation and electron detachment. The potential curve of this state has a minimum at $R = 4.52$ au and crosses the repulsive Be₂ ground-state curve near 5.9 au; for longer R values, Be₂⁻ is unstable with respect to electron loss. The vertical electron detachment energy of Be₂⁻ was predicted to be 0.38 eV.

CONCLUSION

Since 1968 a great deal of progress has been made toward understanding the stability and bonding characteristics of small anions in the gas phase. Quantum chemical methods that adequately treat electron correlation and orbital relaxation effects have been shown to be useful tools for investigating anions. A third-order treatment of correlation seems to be accurate to ± 0.2 eV; second-order calculations are not useful because they have an accuracy of ± 0.6 eV. Koopmans' theorem or Δ SCF-level electron affinities are generally not of sufficiently high accuracy to be useful, although the shapes of SCF-level potential energy surfaces may not be any worse for anions than for neutral molecules. A good choice of basis set, with sufficient diffuse functions, is an essential ingredient of any reasonable calculation on a negative ion. With a flexible basis and a method for treating correlation and relaxation effects one can, as has been demonstrated in the work reviewed here, reliably carry out good quantum mechanical studies of stable negative molecular ions.

In the opinion of this reviewer, the challenges of the immediate future are as follows:

1. the accurate, physically clear, and computationally tractable treatment of metastable negative molecular ions;

2. extension of the work described in this review to anions involving more complex functional groups and the study of substituent effects;
3. development of accurate models that include the effects of solvents so that hydrated gas-phase ions and anions in solution can be quantitatively investigated.

ACKNOWLEDGMENTS

The author acknowledges the financial support of the U.S. Army Research Office (Grant #DAAG-29-74-G-022) and of the National Science Foundation (Grant #CHE 75-19376).

He also thanks Professor Ken Jordan, Dr. George Purvis, and Professor Yngve Öhrn for many helpful discussions.

Literature Cited

1. Berry, R. S. 1969. *Chem. Rev.* 69:533-42
2. Smith, W. D., Chen, T. T., Simons, J. 1974. *Chem. Phys. Lett.* 27:499-502
3. Branscomb, L. M. 1966. *Phys. Rev.* 148:11-18
4. Hotop, H., Patterson, T. A., Lineberger, W. C. 1974. *J. Chem. Phys.* 60:1806-12
5. Pekeris, C. L. 1958. *Phys. Rev.* 112:1649-58
6. Weiss, A. W. 1968. *Phys. Rev.* 166:70-74
7. Clementi, E., McLean, A. D. 1964. *Phys. Rev. A* 133:419-23; Clementi, E., McLean, A. D., Raimondi, D. L., Yoshimine, M. 1964. *Phys. Rev. A* 133:1274-79; Clementi, E. 1964. *Phys. Rev. A* 135:980-84
8. Sinanoglu, O., Oksuz, I. 1968. *Phys. Rev. Lett.* 21:507-11
9. Taylor, H. S., Harris, F. E. 1963. *J. Chem. Phys.* 39:1012-16
10. Wahl, A. C., Gilbert, T. L. 1965. *Bull. Am. Phys. Soc.* 10:1097; Zemke, W. T., Das, G., Wahl, A. C. 1972. *Chem. Phys. Lett.* 14:310-14
11. Cade, P. E. 1967. *J. Chem. Phys.* 47:2390-2406; 1967. *Proc. R. Soc. London Ser. A* 91:842
12. Simons, J., Smith, W. D. 1973. *J. Chem. Phys.* 58:4899-4907
13. Simons, J. 1974. *Chem. Phys. Lett.* 25:122-28
14. Jordan, K. D., Chen, T. T., Simons, J. 1976. *Chem. Phys.* 14:145-47
15. Jørgensen, P., Simons, J. 1975. *J. Chem. Phys.* 63:5302-4
16. Cederbaum, L. S. 1973. *Theor. Chim. Acta* 31:239-60; Cederbaum, L. S., Holneicher, G., Peyerimhoff, S. 1971. *Chem. Phys. Lett.* 11:421-24; Cederbaum, L. S., Holneicher, G., von Niessin, W. 1973. *Chem. Phys. Lett.* 18:503-8
17. Pickup, B. T., Goscinski, O. 1973. *Mol. Phys.* 26:1013-35
18. Purvis, G., Öhrn, Y. 1974. *J. Chem. Phys.* 60:4063-69; Purvis, G., Öhrn, Y. 1975. *J. Chem. Phys.* 62:2045-49
19. Tsui, F., Freed, K. F. 1975. *Chem. Phys. Lett.* 32:345-50
20. Griffing, K., Simons, J. 1975. *J. Chem. Phys.* 62:535-40
21. Kenney, J., Simons, J. 1975. *J. Chem. Phys.* 62:592-99
22. Griffing, K., Simons, J. 1976. *J. Chem. Phys.* 64:3610-14
23. Andersen, E., Simons, J. 1976. *J. Chem. Phys.* 64:4548-50
24. Griffing, K., Kenney, J., Simons, J., Jordan, K. D. 1975. *J. Chem. Phys.* 63:4073-75
25. Jordan, K. D., Griffing, K. M., Kenney, J., Andersen, E. L., Simons, J. 1976. *J. Chem. Phys.* 64:4730-40
26. Andersen, E., Simons, J. Submitted to *J. Chem. Phys.*
27. Carlsten, J. L., Peterson, J. R., Lineberger, W. C. 1976. *Chem. Phys. Lett.* 37:5-8
28. Clementi, E., McLean, A. D. 1963. *J. Chem. Phys.* 39:323-25
29. Boyd, D. B., Lipscomb, W. N. 1967. *J. Chem. Phys.* 46:910-19
30. Krauss, M. 1964. *J. Res. Natl. Bur. Stand.* 63A:635-39; Krauss, M., Neumann, D., Wahl, A. C., Das, G., Zemke, W. 1973. *Phys. Rev. A* 7:69-77
31. Heaton, M. M., Pipano, A., Kaufman, J. J. 1972. *Int. J. Quantum Chem. Symp.* 6:181-86
32. Kari, R. E., Csizmadia, I. G. 1972. *J. Chem. Phys.* 56:4337-44; Robb, M. A., Csizmadia, I. G. 1971. *Int. J. Quantum Chem.* 5:605-35

33. Pfeiffer, G. V. 1967. Unpublished data, Princeton University
34. Popkie, H. E., Henneker, W. H. 1971. *J. Chem. Phys.* 55:617-28
35. McLean, A. D., Yoshimine, M. 1967. *J. Chem. Phys.* 46:3682-83; McLean, A. D., Yoshimine, M., 1967. *Int. J. Quantum Chem.* 15:313-19
36. Gilbert, T. L., Wahl, A. C. 1965. *Bull. Am. Phys. Soc.* 10:1097
37. Fink, W. H., Allen, L. C. Unpublished data
38. Geller, M., Sachs, L., Kaufman, J. J. Unpublished data, RIAS and Jet Propulsion Lab.
39. Thulstrup, P. W., Thulstrup, E. W., Andersen, A., Öhrn, Y., 1974. *J. Chem. Phys.* 60:3975-80
40. Peyerimhoff, S. D., Buenker, R. J., Allen, L. C. 1966. *J. Chem. Phys.* 45:734-49
41. Heaton, M., Cowdry, R. 1975. *J. Chem. Phys.* 62:3002-9
42. Pearson, P. K., Schaefer, H. F. III, Richardson, J. H., Stephenson, L. M., Brauman, J. I. 1974. *J. Am. Chem. Soc.* 96:6778-79
43. Linderberg, J., Öhrn, Y. 1967. *Chem. Phys. Lett.* 1:295-96
44. Linderberg, J., Öhrn, Y. 1972. *Propagators in Quantum Chemistry*. London: Academic.
45. Doll, J. D., Reinhardt, W. P. 1972. *J. Chem. Phys.* 57:1169-84
46. Schneider, B., Taylor, H. S., Yaris, R. 1970. *Phys. Rev. A* 1:855-67; Yarlaga-gadda, B. S., Csanak, G., Taylor, H. S., Schneider, B., Yaris, R. 1973. *Phys. Rev. A* 7:146-54
47. Goscinski, O., Lukman, B. 1970. *Chem. Phys. Lett.* 7:573-76
48. Rowe, D. J. 1968. *Rev. Mod. Phys.* 40:153-66; Rowe, D. J. 1968. *Phys. Rev.* 175:1283-92
49. Purvis, G., Öhrn, Y. 1975. *Chem. Phys. Lett.* 33:396-98
50. Redmon, L. T., Purvis, G., Öhrn, Y. 1975. *J. Chem. Phys.* 63:5011-17
51. Brandow, B. H. 1967. *Rev. Mod. Phys.* 39:771-828
52. Jørgensen, P., Purvis, G. *J. Chem. Phys.* 1977. In press
53. Cade, P. E. 1967. *J. Chem. Phys.* 47:2390-2406
54. Cade, P. E., Huo, W. M. 1967. *J. Chem. Phys.* 47:614-48
55. Herzberg, G. 1961. *Spectra of Diatomic Molecules*, 2nd ed. Princeton: Van Nostrand, p. 508
56. Gaydon, A. G. 1968. *Dissociation Energies and Spectra of Diatomic Molecules*, 3rd ed. London: Chapman & Hall, p. 264
57. Feldmann, D. Private communication
58. Roetti, C., Clementi, E. 1974. *J. Chem. Phys.* 60:4725-29
59. Jensen, D. E., 1970. *J. Chem. Phys.* 52:3305-6; Srivastava, R. D., Uy, O. M., Farber, M., 1971. *Trans. Faraday Soc.* 67:2941-44
60. Berkowitz, J., Chupka, W. A., Walter, T. A. 1969. *J. Chem. Phys.* 50:1497-1500
61. Clementi, E. 1963. *J. Chem. Phys.* 38:996-1000
62. Das, G. 1967. *J. Chem. Phys.* 46:1568-79
63. Herzberg, G. 1961. *Spectra of Diatomic Molecules*, 2nd ed. Princeton: Van Nostrand, p. 546
64. Khrustov, V. F., Stepanov, N. F., Yarovoy, S. S., Abramnikov, A. V., Poshunyaite, N. P., Tsiur, Z. Y. 1971. *Vestn. Mosk. Univ. Khim.* 12:221-23
65. Velasco, R., Ottinger, C., Zare, R. N. 1969. *J. Chem. Phys.* 51:5522-32
66. Patterson, T. A., Hotop, H., Kasdan, A., Norcross, D. W., Lineberger, W. C. 1974. *Phys. Rev. Lett.* 32:189-92
67. Blustin, P. H., Linnett, J. W. 1974. *J. Chem. Soc. Faraday Trans. 2*, 70:826-36
68. Henderson, G. A., Zemke, W. T., Wahl, A.C. 1973. *J. Chem. Phys.* 58:2654-56
69. Bottcher, C., Dalgarno, A. 1975. *Chem. Phys. Lett.* 36:137-44
70. Griffing, K. M., Kenney, J., Simons, J., Jordan, K. D. 1975. *J. Chem. Phys.* 63:4073-75
71. Wallis, R. F., Herman, R., Milnes, H. W. 1960. *J. Mol. Spectrosc.* 4:51-74
72. Crawford, O. H. 1967. *Proc. Phys. Soc.* 91:279-84
73. Coulson, C. A., Walmsley, M. 1967. *Proc. Phys. Soc. London* 91:31-32
74. Crawford, O. H., Koch, B. J. D. 1974. *J. Chem. Phys.* 60:4512-19
75. Garrett, W. R. 1971. *Phys. Rev. A* 3:961-72
76. Turner, J. E., Anderson, V. E., Fox, K. 1968. *Phys. Rev.* 174:81-89
77. Jordan, K. D., Luken, W. 1976. *J. Chem. Phys.* 64:2760-66
78. Yoshimine, M. 1964. *J. Chem. Phys.* 40:2970-76; Yoshimine, M. 1968. *J. Phys. Soc.* 25:1100-19
79. Andersen, E. A. Unpublished data
80. Hehre, W. J., Lathan, W. A., Ditchfield, R., Newton, M. D., Pople, J. A. 1976. *Quantum Chem. Program Exch. program* 236, Indiana Univ.
81. Jordan, K. D., Kinsey, J. L., Silbey, R. 1974. *J. Chem. Phys.* 61:911-17; Jordan, K. D. 1975. *J. Mol. Spectrosc.* 56:329-31
82. Docken, K. K., Hinze, J. 1972. *J. Chem. Phys.* 57:4928-36
83. Steiner, B. 1968. *J. Chem. Phys.* 49:5097-5104

84. Thulstrup, P. W., Thulstrup, E. W. 1974. *Chem. Phys. Lett.* 26:144-48
85. O'Hare, P. A. G. 1971. *J. Chem. Phys.* 54:4124-26; O'Hare, P. A. G., Wahl, A. C. 1970. *J. Chem. Phys.* 53:2834-46; *ibid* 1971. 54:4563-77
86. Cederbaum, L. 1973. *Theor. Chim. Acta* 31:239-60
87. Smyth, K. C., Brauman, J. I. 1972. *J. Chem. Phys.* 56:4620-25; Celotta, R. J., Bennett, R. A., Hall, J. L. 1974. *J. Chem. Phys.* 60:1740-45
88. Richardson, J. H., Stephenson, L. M., Brauman, J. I. 1974. *Chem. Phys. Lett.* 25:318-20
89. Herbst, E., Patterson, T. A. Lineberger, W. C. 1974. *J. Chem. Phys.* 61:1300-4
90. Jordan, K. D. 1976. *J. Chem. Phys.* 65:1214-15, and private communication
91. Burrow, P. D., Jordan, K. D. 1975. *Chem. Phys. Lett.* 36:594-98; Jordan, K. D., Burrow, P. D., Michejda, J. A. 1976. *J. Am. Chem. Soc.* 98:1295-96
92. Jordan, K. D. 1977. *Chem. Phys. Lett.* In press
93. Jordan, K. D., Simons, J. 1976. *J. Chem. Phys.* 65:1601
94. Dixon, D. A., Gole, J. L., Jordan, K. D. Unpublished